Bithiophene−Perfluorobenzene Copolymers

Yongfeng Wang and Mark D. Watson*

Department of Chemistry, University of Kentucky, Lexington, Kentucky 40506-0055

Received June 22, 2008; Revised Manuscript Received September 16, 2008

ABSTRACT: A series of copolymers of 3,3′-dialkylbithiophenes and tetrafluorobenzene units are reported along with non-fluorinated controls. All are characterized by NMR, gel permeation chromatography, differential scanning calorimetry, optical spectroscopy, and wide-angle X-ray diffraction (WAXD). The fluorine substituents enhance backbone planarity, order, and π-stacking in the solid-state as revealed by optical spectroscopy and WAXD. Peak oxidation potential is also increased by 0.55 V relative to a benchmark polymeric semiconductor, poly(3-hexylthiophene). Head-to-head 3-alkylthiophene linkages do not preclude backbone planarity provided the side chains are not too bulky.

Introduction

A general design to improve upon the good performance of regioregular poly(3-hexylthiophene) (rrP3HT)[1] as the active component in organic thin film transistors (OTFT) is emerging. The basic design (Chart 1) incorporates non-alkylated aryl units into polymer backbones between 4,4′-dialkylbithiophene units. This serves two functions: (1) decrease side-chain substitution frequency along the backbone, enhancing long-range order via interdigitation of side chains from adjacent polymers; (2) increase ionization energy (IE) relative to rrP3HTs, thus increasing device stability under ambient conditions.

Groups that have been inserted include unsubstituted bithiophene units, thienothiophene, dithienothiophene, benzodithiophene, and thiazolothiazole (Chart 1).[2] In all these cases, the ionization potential, as estimated electrochemically or by UPS, increased by 0.1−0.3 eV relative to that of rrP3HT. The benzodithiophene derivative is the exception to criterion 1 above, but it meets criterion 2. Long-range ordering is typically observed in these polymers by wide-angle X-ray diffraction (WAXD). In one case, the ordering was so dramatically improved in thin films that AFM images revealed[3] "large" terraces reminiscent of those seen on the surfaces of crystals grown from small molecules, allowing highly detailed clarification[4] of the packing motif. While solid-state packing is one of the most important factors determining device performance, good OTFT performance has been obtained from thiophene-based polymers despite short-range order.[5] This has been specifically demonstrated in the case of photovoltaic devices (PVD) where the more poorly ordered of a pair of constitutionally similar thiophene-based polymers gave better performance.[6]

Incorporation of tetrafluorobenzene (TFB) units as "π" in the generic structure depicted in Chart 1 meets the two criteria described above, with an additional feature: combinations of fluorinated (πF) and non-fluorinated (π) pi-electron systems enforce face-to-face π-stacking.[7] Innumerable crystallographic examples bear this out, including $\pi-\pi$F systems composed of thiophenes and fluorinated benzenes.[8] Although random incorporation of varying levels of TFB units into a P3HT did not lead to enhanced order, IE increased by up to 0.3 eV with increasing TFB loading.[9] A series of alternating copolymers of benzene and alkylated *terthiophenes* or *quaterthiophenes* were reported.[10] In some cases fluorine substituents on the benzene rings increased oxidation potential and enhanced ordering.

We describe here the synthesis and initial structure−property studies of alternating TFB−*bithiophene* copolymers fitting the two design principles described above. We employ bithiophene units with head-to-head (HH), rather than tail-to-tail (TT), alkyl substitution to minimize steric interaction with pendant fluorine atoms that would preclude backbone planarization. Despite the fact that a HH−TT polyalkylthiophene was shown conclusively to be quite nonplanar,[11] HH units should not intrinsically preclude coplanarity of bithiophene repeat units as clearly illustrated both by small-molecule crystallographic studies[12] and indirectly by optical measurements of conjugated polymers. Backbone coplanarity is more likely dependent on regularity of the spacing of the side chains along the backbone, commensurate space-filling demands of side chains with planarized backbones, and any additional driving force such as donor−acceptor interactions. For example, within a pair of poly(terthiophenes) bearing two alkyl substituents per repeat, TT substitution gave a more planarized backbone.[2d] However, the HH version of a pair of dialkylbithiophene−benzothiadiazole copolymers was more planarized than the TT version as indicated by reduced optical band gap.[13]

The backbone rings of the polymers reported herein can be relatively coplanarized despite their head-to-head thiophene linkages. Coplanarity can be enforced by intermolecular $\pi-\pi$F attractions, with possible contribution from intramolecular sulfur−fluorine[14] interactions, similar to the effect of S−O interactions.[15] The polymers were prepared with three different types of alkyl substituents in order to study the effect of steric bulk on solubility and self-assembly. Non-fluorinated derivatives are prepared as controls. Properties are investigated by differential scanning calorimetry, optical spectroscopy, cyclic voltammetry, and wide-angle X-ray diffraction.

Experimental Section

Materials and Methods. $CHCl_3$ and THF were distilled from appropriate drying agents and stored over molecular sieves under argon. Zinc chloride anhydrous beads were purchased from Aldrich and stored in an argon-filled glovebox. All other materials were used as purchased. Unless otherwise stated, all manipulations and reactions were carried out under argon in a glovebox or using standard Schlenk techniques. ^{1}H, ^{13}C, and ^{19}F NMR spectra were recorded on a Varian INOVA 400 MHz spectrometer (purchased under the CRIF Program of the National Science Foundation, Grant CHE-9974810). Chemical shifts were referenced to residual protio-solvent signals, except for ^{19}F spectra, where CCl_3F was added as internal standard and set to $\delta = 0$ ppm. Relative molecular weight determinations were made using a Waters 600E HPLC system, driven by Waters Empower Software and equipped with two linear mixed-bed GPC columns (American Polymer Standards Corp., AM Gel Linear/15) in series, and refractive index and photodiode array detectors. The system was calibrated with 11

* Corresponding author. E-mail: mdwatson@uky.edu.

10.1021/ma801400v CCC: $40.75
Published on Web 10/28/2008

Chart 1. Structures of Published Bithiophene Copolymers Demonstrating Good to Excellent Performance in OFETs, All with Ambient Stability Superior to P3ATs

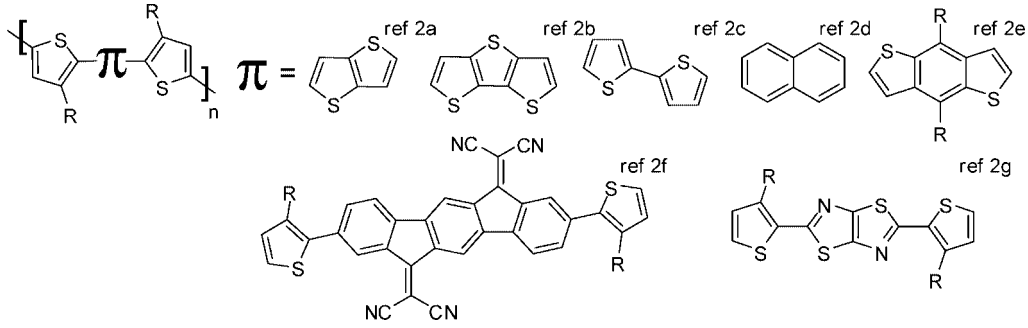

narrow PDI polystyrene samples in the range 580−2 × 10^6 Da with THF at a flow rate of 1 mL/min. Melting points for small molecules and polymers are the peak values measured at a heating rate of 10 or 20 °C/min using a nitrogen-purged Mettler 822^e differential scanning calorimeter. GC-MS data were collected from an Agilent 6890N GC with 5973 MSD. Photoluminescence and UV−vis absorption spectra were recorded on a Fluorolog-3 fluorometer and Varian CARY 1 spectrophotometer, respectively. Electrochemical measurements were performed under nitrogen using a BAS-CV-50W voltammetric analyzer and three-electrode cell (platinum working, silver wire counter, and Ag/AgCl reference electrodes). The supporting electrolyte solution (0.1 M Bu_4NPF_6, anhydrous CH_3CN) was thoroughly purged with N_2 before each measurement, and ferrocene/ferrocenium (Fc/Fc^+, E_{peak} = 0.41 V) was used as internal reference. Polymer fibers were produced by mechanically forcing powdered samples through a thermally equilibrated piston-actuated extruder with 0.5 mm annular die. Detailed procedures for monomer synthesis and their characterization are included in the Supporting Information.

Polymer Synthesis. *Polymer* **1a**. A solution of **3a** (120 mg, 0.207 mmol) in 3 mL of anhydrous chloroform was added dropwise to $FeCl_3$ (134.3 mg, 1.08 mmol) in 10 mL of anhydrous chloroform at RT. The mixture was then heated at 50 °C for 48 h. The blue-black mixture was poured into 150 mL of methanol to generate a blue-green precipitate. The solid was collected by filtration, washed with methanol and water, and then dedoped by stirring with 80 mL of a mixture of concentrated ammonium hydroxide and water (v:v = 3:1) for 1.5 h. A yellow solid was separated by centrifugation and washed with methanol. This solid was dissolved in chloroform and precipitated into 100 mL of methanol. The resulting yellow polymer was stirred in 6 mL of hexane at 60 °C for 6 h to separate lower molecular weight oligomers. After being centrifuged and dried, a yellow solid was obtained (37 mg, 31%). ^{1}H NMR (400 MHz, $CDCl_3$, 55 °C) δ: 7.63 (s, 4H), 7.24 (s, 2H), 2.61 (broad, 4H), 1.86 (broad, 4H), 1.27 (broad, 36H), 0.89 (broad, 6H). ^{13}C NMR (100 MHz, $CDCl_3$, 55 °C): 143.70, 143.41, 133.55, 128.57, 126.01, 124.83, 31.96, 30.71, 29.72, 29.60, 29.48, 29.36, 29.30, 29.24, 22.68, 14.03. M_n(GPC) = 30 kDa (PDI = 1.98).

Polymer **1b**. Synthesized as described for polymer **1a**, substituting room temperature for 50 °C as the polymerization temperature. Polymer **1b** was obtained as a yellow solid in 55% yield. ^{1}H NMR (400 MHz, $C_2D_2Cl_4$, 70 °C) δ: 8.32 (s, 4H), 7.97 (s, 2H), 3.30 (broad, 4H), 2.34−1.79 (m, 20H), 1.51 (broad, 18H). ^{13}C NMR (100 MHz, $C_2D_2Cl_4$, 70 °C): 144.52, 143.61, 133.86, 128.75, 126.36, 125.55, 39.87, 38.52, 37.57, 33.22, 28.54, 27.34, 25.24, 23.01, 22.92, 19.94. M_n(GPC) = 47 kDa (PDI = 1.62).

Polymer **1aF**. Prepared similarly to polymer **1a**, starting from compound **3aF** (100 mg, 0.154 mmol), $FeCl_3$ (100 mg, 4eq), and $CHCl_3$ (20 mL). (68 mg, 67%). ^{1}H NMR (400 MHz, $C_2D_2Cl_4$, 75 °C) δ: 7.63 (s, 2H), 2.70 (broad, 4H), 1.69 (broad, 4H), 1.30 (broad, 36H), 0.92 (broad, 6H). ^{19}F NMR (376 MHz, $C_2D_2Cl_4$, 75 °C) δ: −140.80 (m, 4F), −140.95 (s, 34F), −141.55 (m, 4F). M_n(GPC) = 14 kDa (PDI = 2.55).

Polymer **1bF**. Prepared similarly to polymer **1a**, starting from compound **3bF** (100 mg, 0.168 mmol), $FeCl_3$ (109 mg, 4eq), and $CHCl_3$ (20 mL). Isolated as an orange-red solid (49 mg, 49%). ^{1}H NMR (400 MHz, $C_2D_2Cl_4$, 75 °C) δ: 7.64 (s, 2H), 2.74 (m, 4H), 1.71 (m, 2H), 1.56 (m, 6H), 1.34 (m, 6H), 1.19 (m, 6H), 0.95 (d, J = 6.4 Hz, 6H), 0.91 (d, J = 6.8 Hz, 12H). ^{19}F NMR (376 MHz, $C_2D_2Cl_4$, 75 °C) δ: −140.80 (m, 4F), −140.98 (s, 85F), −141.55 (m, 4F). M_n(GPC) = 22 kDa (PDI = 2.78).

Scheme 1. Synthesis of Monomers and Polymers[a]

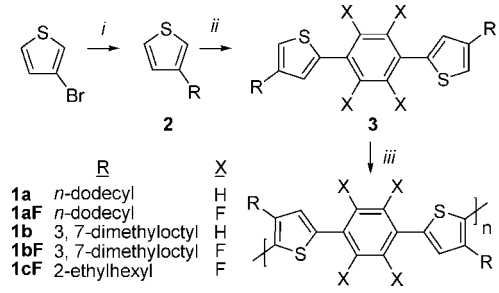

[a] *i*: RMgBr, $NiCl_2$(dppp), ether; *ii:* (a) LDA, THF, −78 °C, (b) $ZnCl_2$, −78 °C → RT, (c) $Pd(PPh_3)_4$, THF, *p*-$Br_2C_6H_4$ or *p*-$Br_2C_6F_4$; *iii:* $FeCl_3$, $CHCl_3$.

Polymer **1cF**. Prepared similarly to polymer **1a**, starting from compound **3cF** (123 mg, 0.228 mmol), $FeCl_3$ (148 mg, 4eq), and $CHCl_3$ (12 mL). Isolated as a yellow solid (70 mg, 57%). ^{1}H NMR (400 MHz, $CDCl_3$, RT) δ: 7.55 (s, 2H), 2.58 (m, 4H), 1.61 (m, 2H), 1.23 (m, 16H), 0.84 (m, 12H). ^{19}F NMR (376 MHz, $C_2D_2Cl_4$, RT) δ: −140.95 (m, 4F), −141.09 (s, 64F), −141.60 (m, 4F). M_n(GPC) = 18 kDa (PDI = 2.89).

Results and Discussion

Monomers were prepared via standard procedures and polymerized by oxidative coupling with $FeCl_3$ (Scheme 1). Polymer characteristics are summarized in Table 1. The effects of fluorination are immediately apparent: The non-fluorinated polymers are yellow solids, while the fluorinated polymers bearing dodecyl and 3,7-dimethyloctyl side chains are orange to red (depending on processing history), indicating increased backbone planarization/π-stacking. The exception is yellow **1cF** bearing more bulky 2-ethylhexyl side chains. The non-fluorinated polymers and **1cF** are readily soluble in common organic solvents at room temperature, while **1aF/1bF** are soluble only with heating.

Optical and Electrochemical Characterization. Solution absorption and PL spectra from polymers **1** are included in Figure 1, and relevant data are collected in Table 1. There is little or no drive toward backbone planarization, and the thermal population of states results in broad featureless optical spectra with similar λ_{max} virtually independent of substitution. The absorption λ_{max} of the non-fluorinated polymers **1a/b** are slightly red-shifted (10−12 nm) compared to the fluorinated ones. The ethylhexyl chains of **1cF** cause a small blue shift in PL (<10 nm). The average λ_{max} values are similar to those reported for

Table 1. Properties of Polymers

polymer	yield(%)	M_n [PDI][a] (kDa)	λ_{max} sol abs[b]/PL[c] (nm)	λ_{max} film[d] abs/PL (nm)	λ_{onset} (abs) sol/film (nm)	E_g[e] sol/film (eV)	T_g[f]/T_m[g] (°C)
1a	31	30 [2.0]	388/486	401/505	443/494	2.80/2.51	52,[f] 115[g]
1aF	67	14 [2.6]	377/485	457/601	437/567	2.84/2.19	107,[g] 149[g]
1b	55	47 [1.6]	390/488	394/505	449/467	2.76/2.66	38[f]
1bF	49	22 [2.8]	380/486	488/612	437/569	2.84/2.18	212[g]
1cF	65	11 [2.1]	377/483	390/544	434/464	2.86/2.67	23[f]

[a] GPC vs polystyrene standards. [b] 10^{-5} M THF. [c] 10^{-7}−10^{-8} M THF. [d] Spin-cast from toluene solution (1 mg/mL). [e] $E_g = 1241/\lambda_{onset}$. [f] DSC: second-order transition. [g] DSC: first-order transition.

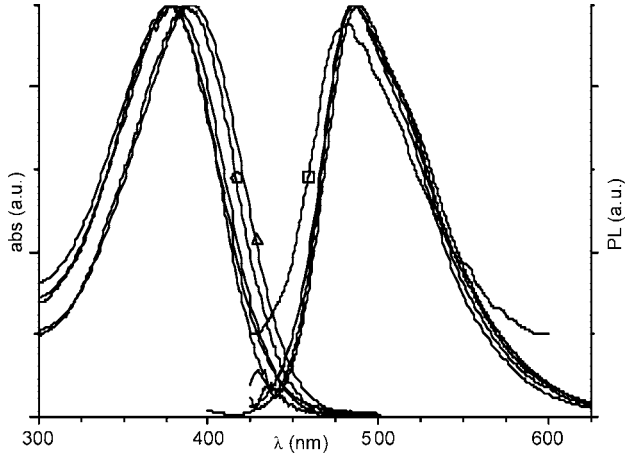

Figure 1. Solution absorption (10^{-5} M THF) and photoluminescence (10^{-7}−10^{-8} M THF) spectra of polymers **1**. All are nearly identical except slight outliers labeled as (○) **1a**, (△) **1b**, and (□) **1cF**.

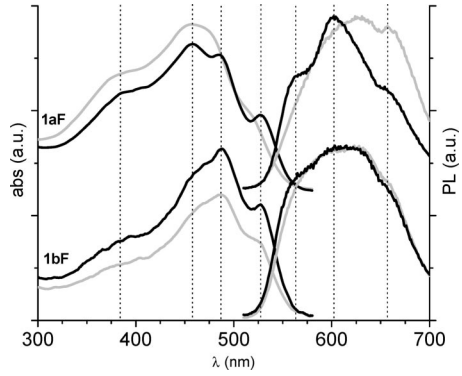

Figure 2. Absorption and photoluminescence spectra from spin-cast films (1 mg/mL toluene) of **1a/bF** measured at RT before (gray) and after (black) annealing 20 °C below their peak melting temperatures.

an analogous non-fluorinated version of **1** carrying hexyl side chains.[16]

Thin film absorption and PL measurements (Figure SI 2) of the non-fluorinated polymers are little changed from those in solution, indicating significant backbone torsion and absence of π-stacking in both states. On the contrary, thin film measurements (Figure 2) of fluorinated **1aF** and **1bF** show relatively large red shifts (e.g., absorption $\Delta\lambda_{max} = 80$ and 108 nm) and fine structure. Skabara et al. reported[10] similar differences between fluorinated and non-fluorinated benzene−terthiophene and −quaterthiophene copolymers carrying hexyl side chains ($\Delta\lambda_{max} = 60$ and 87 nm). These differences are brought about by intermolecular π−πF interactions and/or intramolecular S−F interactions.

Thermal annealing enhances fine structure in the spectra of **1a/1bF**, corresponding to an increase in order and narrowing of the population of states. While the spectra from annealed **1aF** and **1bF** are identical in terms of position of maxima/shoulders (Figure 2, vertical dotted lines), **1aF** undergoes greater changes upon annealing, including a slight red shift and ultimately more developed fine structure. These differences are dictated by the side chains: "crystallizable" *n*-dodecyl chains versus disordered racemic 3,7-dimethyloctyl chains. A low-energy absorption shoulder is present in the spectra of pristine films of both but is more distinct and slightly more red-shifted (10 nm) for **1bF**. After annealing, the shoulders become more distinct and centered at identical wavelength ($\lambda = 528$ nm) for both **1a/1bF**. The absorption λ_{max} of polymer **1cF** undergoes a much smaller red shift on going from solution to the solid state (Figure SI 1). The bulkier 2-ethylhexyl side chains preclude planarization and or π-stacking. All these conclusions are supported below by WAXD studies.

Oxidation potentials of thin films of polymer **1b** and **1bF** were measured by Osteryoung square-wave voltammetry and compared to rrP3HT ($E_{peak} = 0.45$ V vs Fc/Fc^+ in our hands) measured under identical conditions. The peak oxidation potential of **1b** is increased by 0.36 V relative to rrP3HT due to incorporation of backbone benzene rings. TFB further increased the peak oxidation potential by 0.19 V, an overall increase of 0.55 V relative to rrP3HT. Replacement of benzene with TFB in benzene−terthiophene copolymers caused an increase of 0.16V while for benzene−quaterthiophene copolymers the oxidation potential was very slightly decreased, perhaps due to differences in backbone planarity overcoming the direct electronic influence of fluorine substituents.[10]

Wide-Angle X-ray Diffraction (WAXD). Solid state order was investigated by two-dimensional wide-angle X-ray diffraction (2D-WAXD) from mechanically aligned fibers. The fiber samples were mounted perpendicular to the incident X-ray beam, and diffracted X-rays were collected with an area detector (Figure 3, Table 2).

For the polymers **1aF/1bF**, there are series of equatorial reflections at smaller angles with relative *d*-spacings of *L*, *L*/2, *L*/3, and regularly decreasing intensities. These indicate parallel zones of alternating electron density corresponding to polymer backbones separated by alkyl side chains (lamellar packing, with repeating distance = *L*). The lamellar spacing for **1aF** (20 Å) closely matches the space-filling demands of fully interdigitated, ordered all-trans dodecyl chains, which in turn give rise to a series of weak, relatively narrow reflections centered on the meridian. The disordered side chains of **1bF** yield an isotropic halo centered near $d = 4.9$ Å. The side chains of **1bF** are shorter than those of **1aF** by four carbons, but the lamellar spacing is reduced by <2 Å, suggesting that the side chains are less interdigitated due to their greater lateral demand for space. Meridional arcs at $d = 5.6$ Å, approximately 1/2 the length of the **1bF** repeat unit (12.1 Å based on a related small-molecule crystal structure[8a]), suggest face-to-face neighbors pack with fluorinated rings overlying non-fluorinated rings. Weak, diffuse off-meridional intensity maxima within the side-chain halo flank these meridional arcs. This corresponds to a truncated layer line suggesting at least short-range 3-dimensional ordering within the relatively long-range ordered lamella. Perhaps this 3D order can be increased by choosing a πF segment that more closely matches the length of bithiophene units, e.g., perfluoronaphthalene, which we are currently pursuing.

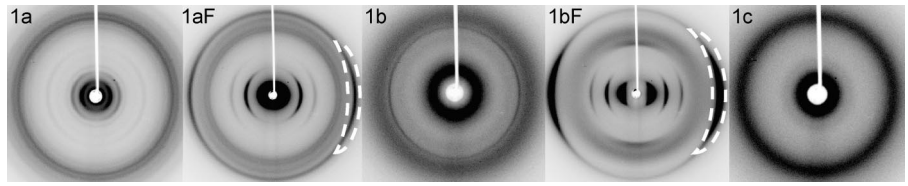

Figure 3. Characteristic 2D WAXD patterns of all newly reported polymers. Fiber axes vertical. Dashed crescents enclose arcs assigned to the π-stacking distance.

Table 2. Data Collected from Diffraction Patterns in Figure 3

polymer	lamellar spacing L, $L/2$, $L/3$ (Å)	π-stacking (Å)	meridional maxima (Å)	"halo" (Å)
1a	23.4, 14.2, etc.[a]		4.6−3.9	
1aF	20.0, 9.9, 6.6	3.5		
1b				13.7, 4.8,[b] 4.2
1bF	18.3, 9.4, 6.2	3.5	5.6	4.93
1cF				19.4, 4.6

[a] Not simple lamellar. [b] Sharp ring likely from residual inorganics.

For both **1a/1bF**, there are intense equatorial reflections (d = 3.5 Å) assigned to the π-stacking distance of the polymer backbones. This spacing is less than typically reported for thiophene-based (co)polymers (3.6−3.9 Å). It is tempting to attribute our closer π-stacking distance to $\pi-\pi$F attraction, but other reported larger values might be overestimated due to backbone ring tilting or offset relative to the stacking axis, similar to "pitch" and "roll" terms describing the crystalline π-stacks of small molecules.[17] These values should then normally be taken as upper limits. The contrast of diffractograms was notably increased upon thermal annealing as expected from optical measurements described above.

The differing degrees to which the absorption and PL spectra of solution-cast films from polymers **1a/1bF** change upon annealing can now be explained in terms of side-chain ordering. The disordered side chains of **1bF** are simply space-filling spectators, which allow packing to be dominated by the main chains. The as-cast state of order more closely resembles the equilibrium state obtained upon annealing. However, the equilibrium state of polymer **1aF** requires cooperative ordering of main and side chains, which is less likely to be achieved during rapid solvent evaporation.

In the diffractogram from **1cF**, there are just two radially symmetric reflections corresponding to the average distances separating disordered main and side chains. Polymer **1cF** is therefore completely amorphous. The radial symmetry of these reflections indicates that any alignment from extrusion was lost prior to WAXD measurements due to a low glass transition temperature. The racemic 2-ethylhexyl side chains present significantly greater steric bulk in the vicinity of the polymer backbone, disrupting ordering and precluding π-stacking/planarization. This again agrees with the solid-state optical measurements and the polymer's color (yellow vs orange to red for polymers **1a/1bF**). A recent report[18] reveals that regioregular poly-3-ethylhexylthiophene is also amorphous, in contrast to highly ordered rrP3HTs bearing n-alkyl chains.

Diffraction patterns of ordered **1bF** and amorphous **1b** carrying identical side chains clearly reveal the effect of TFB on solid-state packing. Recall that the optical spectra of **1bF** undergo significant red shifts upon going from solution to solid state, while those of **1b** are relatively unchanged. The WAXD pattern of **1b** reveals that it is both completely amorphous and unoriented, in agreement with DSC measurements which revealed only a glass transition (38 °C).

Concluding Remarks. Fluorine substituents on the benzene rings of alternating copolymers with 3,3′-dialkylbithiophene units enhance order, backbone planarization, and π-stacking in the solid state. These changes arise from attractive intermolecular $\pi-\pi$F and/or intramolecular S−F interactions. Head-to-head substitution of the bithiophene units does not interfere, provided that the side chains are not too bulky. A backbone spacer (C_6F_4) between the bithiophene units allows for full interdigitation of dodecyl side chains within lamella and substantially increases oxidation potential (and therefore ionization energy) relative to P3HT. These are features which have led to higher and more stable performance of bithiophene-based copolymers as p-type semiconductors in thin-film transistors in ambient atmosphere.

Acknowledgment. We thank the National Science Foundation (CHE 0616759) for financial support. Y.W. acknowledges a Kentucky Opportunity Graduate Fellowship. rrP3HT was provided by Dean M. DeLongchamp of NIST.

Supporting Information Available: Experimental procedures, spectroscopic data, and analytical data. This material is available free of charge via the Internet at http://pubs.acs.org.

References and Notes

(1) Sirringhaus, H.; Brown, P. J.; Friend, R. H.; Nielsen, M. M.; Bechgaard, K.; Langeveld-Voss, B. M. W.; Spiering, A. J. H.; Janssen, R. A. J.; Meijer, E. W.; Herwig, P.; de Leeuw, D. M. *Nature (London)* **1999**, *401*, 685–8.

(2) (a) McCulloch, I.; Heeney, M.; Bailey, Cl; Genevicius, K.; MacDonald, I.; Shkunov, M.; Sparrowe, D.; Tierney, S.; Wagner, R.; Zhang, W.; Chabinyc, M. L.; Kline, R. J.; McGehee, M. D.; Toney, M. F. *Nat. Mater.* **2006**, *5*, 328–33. (b) Li, J.; Qin, F.; Li, C. M.; Bao, Q.; Chan-Park, M. B.; Zhang, W.; Qin, J.; Ong, B. S. *Chem. Mater.* **2008**, *20*, 2057–9. (c) Ong, B. S.; Wu, Y.; Gardner, S. *J. Am. Chem. Soc.* **2004**, *126*, 3378–9. (d) McCulloch, I.; Bailey, C.; Giles, M.; Heeney, M.; Love, I.; Shkunov, M.; Sparrowe, D.; Tierney, S. *Chem. Mater.* **2005**, *17*, 1381–5. (e) Pan, H.; Li, Y.; Wu, Y.; Liu, P.; Ong, B. S.; Zhu, S.; Su, G. *J. Am. Chem. Soc.* **2007**, *129*, 4112–3. (f) Usta, H.; Facchetti, A.; Marks, T. J. *J. Am. Chem. Soc.* **2008**, 000ASAP doi 10.1021/ja802266u. (g) Osaka, I.; Sauve, G.; Zhang, R.; Kowalewski, T.; McCullogh, R. D. *Adv. Mater.* **2007**, *19*, 4160–5.

(3) Kline, R. J.; DeLongchamp, D. M.; Fischer, D. A.; Lin, E. K.; Richter, L. J.; Chabinye, M. L.; Toney, M. F.; Heeney, M.; McCulloch, I. *Macromolecules* **2007**, *40*, 7960–5.

(4) Delongchamp, D. M.; Kline, R. J.; Lin, E. K.; Fischer, D. A.; Richter, L. J.; Lucas, L. A.; Heeney, M.; McCulloch, I.; Northrup, J. E. *Adv. Mater.* **2007**, *19*, 833–7.

(5) Zhang, M.; Tsao, H. N.; Pisula, W.; Yang, C.; Mishra, A. K.; Muellen, K. *J. Am. Chem. Soc.* **2007**, *129*, 3472–3.

(6) Thompson, B. C.; Kim, Bumjoon, J.; Kavulak, D. F.; Sivula, K.; Mauldin, C.; Frechet, J. M. J. *Macromolecules* **2007**, *40*, 7425–8.

(7) (a) Patrick, C. R.; Prosser, G. S. *Nature (London)* **1960**, *187*, 1021. (b) Bacchi, S.; Benaglia, M.; Cozzi, F.; Demartin, F.; Filippini, G.; Gavezzotti, A. *Chem.—Eur. J.* **2006**, *12*, 3538–46. (c) Reichenbaecher, K.; Suess, H. I.; Hulliger, J. *Chem. Soc. Rev.* **2005**, *34*, 22–30.

(8) (a) Yoon, M.-H.; Facchetti, A.; Stern, C. E.; Marks, T. J. *J. Am. Chem. Soc.* **2006**, *128*, 5792–01. (b) Crouch, D. J.; Skabara, P. J.; Heeney, M.; McCulloch, I.; Coles, S. J.; Hursthouse, M. B. *Chem. Commun.* **2005**, 1465–7. (c) Wang, Y.; Parkin, S. R.; Watson, M. D. *Org. Lett.* **2008**, *10*, 4421–24.

(9) Sainova, D.; Janietz, S.; Asawapirom, U.; Romaner, L.; Zojer, E.; Koch, N.; Vollmer, A. *Chem. Mater.* **2007**, *19*, 1472–81.

(10) Crouch, D. J.; Skabara, P. J.; Lohr, J. E.; McDouall, J. J. W.; Heeney, M.; McCulloch, I.; Sparrowe, D.; Shkunov, M.; Coles, S. J.; Horton, P. N.; Hursthouse, M. B. *Chem. Mater.* **2005**, *17*, 6567–78.

(11) Maior, R.M. S.; Hinkelman, K.; Eckert, H.; Wudl, F. *Macromolecules* **1990**, *23*, 1268–79.

(12) Compare (non)planarized structures in: (a) Barbarella, G.; Zambianchi, M.; Bongini, A.; Antolini, L. *Adv. Mater.* **1992**, *4*, 282–5. (b) Barbarella, G.; Zambianchi, M.; Antolini, L.; Ostoja, P.; Maccagnani, P.; Bongini, A.; Marseglia, E. A.; Tedesco, E.; Gigli, G.; Cingolani, R. *J. Am. Chem. Soc.* **1999**, *121*, 8920–8926.
(13) Jayakannan, M.; Van Hal, P. A.; Janssen, R. A. J. *J. Polym. Sci., Part A: Polym. Chem.* **2002**, *40*, 251–61.
(14) (a) Wang, Y.; Parkin, S. R.; Gierschner, J.; Watson, M. D. *Org. Lett.* **2008**, *10*, 3307–10. (b) Subramanian, S.; Park, S. K.; Parkin, S. R.; Podzorov, V.; Jackson, T. N.; Anthony, J. E. *J. Am. Chem. Soc.* **2008**, *130*, 2706–7.
(15) (a) Irvin, J. A.; Schwendeman, I.; Lee, Y.; Abboud, K. A.; Reynolds, J. R. *J. Polym. Sci., Part A: Polym. Chem.* **2001**, *39*, 2164–78. (b) Pomerantz, M. *Tetrahedron Lett.* **2003**, *44*, 1563–65.
(16) Pei, J.; Yu, W.-L.; Huang, W.; Heeger, A. J. *Macromolecules* **2000**, *33*, 2462–71.
(17) Curtis, M. D.; Cao, J.; Kampf, J. W. *J. Am. Chem. Soc.* **2004**, *126*, 4318–4328.
(18) Zhang, Y.; Tajima, K.; Hirota, K.; Hashimoto, K. *J. Am. Chem. Soc.* **2008**, *130*, 7812–3.

MA801400V